

## OPTICAL CHARACTERIZATION OF STRAINS IN ALN/GAN HETEROSTRUCTURES

*V.V. Zalamai (a), V.V. Ursaki (a), I.M. Tiginyanu (a), N.N. Syrbu (a),  
S. Hubbard (b), D. Pavlidis (b), A. Ghicov (a)*

*(a) Laboratory of Low-Dimensional Semiconductor Structures, Institute of  
Applied Physics, Technical University of Moldova, MD-2004 Chisinau,  
Moldova*

*(b) EECS Department, The University of Michigan, Ann Arbor, Michigan 48109-  
2122, USA*

Strains in AlN/GaN/sapphire heterostructures were characterized using photoreflectivity (PR) and photoluminescence (PL) spectroscopy. The growth of an  $\sim 20$  nm thick GaN nucleation layer between the sapphire substrate and the  $1.3\ \mu\text{m}$  thick GaN channel layer was found to reduce the strain in the GaN layer by 50%. The remaining strain was shown to increase the  $\Delta E_{\text{BA}}$  and  $\Delta E_{\text{CA}}$  exciton splitting by a factor of 8/5 in comparison with non-stressed material. The activation energy of the A and B excitons equals 26 meV and is independent of strains.

Keywords: GaN-AlN heterostructures; Photoluminescence, Photorefectance;  
Excitons, Strains.

Pacs: 78.40.Fy; 78.55.Cr; 78.66.Fd.

### 1. INTRODUCTION.

GaN and related alloys are presently the most attractive materials for high-efficiency light emitting devices in the ultraviolet and blue energy region [1,2] as well as for high-power microwave devices [3] and field-effect transistors [4]. Particularly, AlN, with its relatively high dielectric constant (8.5) and wide-bandgap (6.2 eV), has the potential to be an excellent choice for the gate dielectric in GaN based MISFET devices [5,6]. Due to the lack of suitable nitride substrate material, heteroepitaxial growth on sapphire or 6H-SiC substrates is actually common practice. The large lattice and thermal mismatches between GaN and these materials result in residual strain in the heterostructures that can seriously influence the device quality. On the other hand, as it is well known, the strain-induced effects can become an advantage for achieving desirable device parameters [7]. For instance, the photoluminescence peak position can be shifted hundreds of meV by varying the strain in QWs. Thus, strain engineering is a tool to achieve long wavelength emitters when the use of active layers with high indium content in InGaN based QWs is undesirable [8]. In order to design high-quality low-dislocation density GaN and AlN-based films and devices, the knowledge of strain is essential. The common practice to reduce the strain in GaN layers when necessary is the growing of a buffer layer. In spite of that, in many cases the remaining amount of strain is considerable. Optical spectroscopy is a highly useful tool to study many important material properties, strains, defects formed at the interfaces etc [9]. In particular, it is important to understand the impact of strains

to excitons in photoluminescence since the photonic devices are based on emission phenomena. These issues are especially important in the realization of exciton-based photonic devices since the nature of the band edge PL recombination processes was shown to be excitonic up to room temperature [10]. The impact of biaxial strain on the exciton resonance energies and the band structure of wurtzite GaN was extensively studied both theoretically [11-17] and experimentally [14-27]. The strain induce shift of the excitonic photoluminescence and reflectivity lines was established experimentally [16, 20-25]. Excitonic energy splitting  $\Delta E_{BA}$  in GaN layers grown on sapphire substrates was found to exhibit a weak sublinear dependence on strain, while  $\Delta E_{CA}$  dependence is superlinear [16,22]. The accumulated experimental data allow one to reliably characterize strains in GaN layers through the position of excitonic lines in optical spectra.

The goal of the following paper is to make use of optical methods for the characterization of stresses in GaN layers of AlN/GaN/sapphire heterostructures.

## 2. EXPERIMENTAL DETAILS.

The GaN and AlN layers were grown by low-pressure (60-110 Torr) MOCVD on c-plane (0001)sapphire substrates. Standard precursors of trimethylgallium (TMGa), trimethylaluminum (TMAI), and ammonia (NH<sub>3</sub>) were used as alkyl and hydride sources. The alkyl and hydride sources were kept separate until just before the quartz reactor. The carrier gas was Pd-cell purified hydrogen (H<sub>2</sub>). Heating was accomplished by RF induction of the graphite susceptor. All switching of valves and manifolds was done using computer control.

The sapphire substrates were initially cleaned in TCE, ACE, IPA, and H<sub>2</sub>SO<sub>4</sub>/H<sub>3</sub>PO<sub>4</sub>. After a high-temperature (1200 C) cleaning in H<sub>2</sub>, the growth temperature was lowered to 500 C. Nitridation was performed and then an ~20 nm thick GaN nucleation layer was grown. After ramping the temperature to 1000 C, a 1.3  $\mu$ m unintentionally doped (UID) GaN channel layer was grown. The AlN layers were grown with thickness ranging from 3–35 nm.

The quality of the GaN layer and the presence of the AlN thin film were confirmed using a High-resolution X-ray Diffractometer (HRXRD). The XRD scans have shown distinct (0002) GaN and AlN peaks. The FWHM of the GaN peak was ~120 arcsec, indicating the GaN channel layer of good quality.

The photorefectivity was measured using the light from a halogen lamp. The reflected white light from the sample was analyzed through a double spectrometer with 1200 lines/mm gratings assuring a linear dispersion of 0.8 nm/mm. The signal from a FEU-106 photomultiplier with SbKNaCs photocathode working in a photon counting mode was introduced in an IBM computer via the IEEE-488 interface for further data processing. The photoluminescence was excited by the 334 nm line of an Ar<sup>+</sup> Spectra Physics laser and analyzed with the same experimental set-up. The resolution was better than 0.5 meV in both PR and PL experiments. The samples were mounted on the cold station of a LTS-22-C-330 workhorse-type optical cryogenic system.

## 3. RESULTS AND DISCUSSIONS.

Fig. 1. illustrates typical reflectivity and photoluminescence spectra of GaN channel layers. The reflectivity spectrum consists of two major features related to the  $X_A^{n=1}$  and  $X_B^{n=1}$  excitons ground states as well as weak features at higher energies associated with  $X_A^{n=2}$  and  $X_B^{n=2}$  excited states and the ground state of the

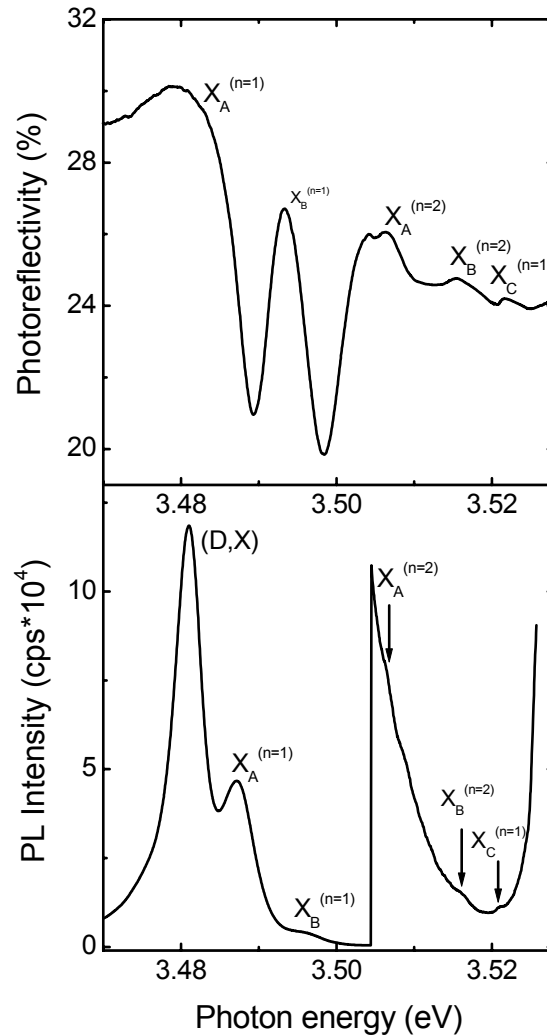


Fig. 1. Typical reflectivity (a) and photoluminescence (b) spectrum of a GaN channel layer measured at 10 K.

$X_C^{n=1}$  exciton. The luminescence spectrum is absolutely predominated by the  $D^0X$  bound exciton [28],  $X_A^{n=1}$  and  $X_B^{n=1}$  excitonic emission. Very weak features corresponding to  $X_A^{n=2}$ ,  $X_B^{n=2}$  and  $X_C^{n=1}$  resonance are as well observed between the sharp decrease of the  $X_B^{n=1}$  luminescence from one side and a sharp increase of the signal due to the 351 nm laser plasma line from the other side. The position of the  $D^0X$  (1.481 eV),  $X_A^{n=1}$  (1.487 eV) and  $X_B^{n=1}$  (1.495 eV) peaks in the luminescence spectrum are shifted by  $\sim 10$  meV toward high energies in comparison with the position of respective excitons in non-stressed GaN layers grown on GaN substrates [10,29]. It means that considerable strains remain in the GaN channel layer due to the mismatches between the layer and sapphire substrate. According to [27], the  $D^0X$  luminescence peak is shifted by about 20 meV toward high energy for a GaN layer of a similar thickness grown on sapphire substrate without any buffer layer. One can deduce that the nucleation GaN layer twice reduces the strains. The remaining strains can be estimated using the previously reported rates of the exciton line shifts with the biaxial stress in GaN layers. Mainly two values were reported: about 20 meV/GPa [21,24,25] and 40 meV/GPa [20,22,23]. Therefore, one

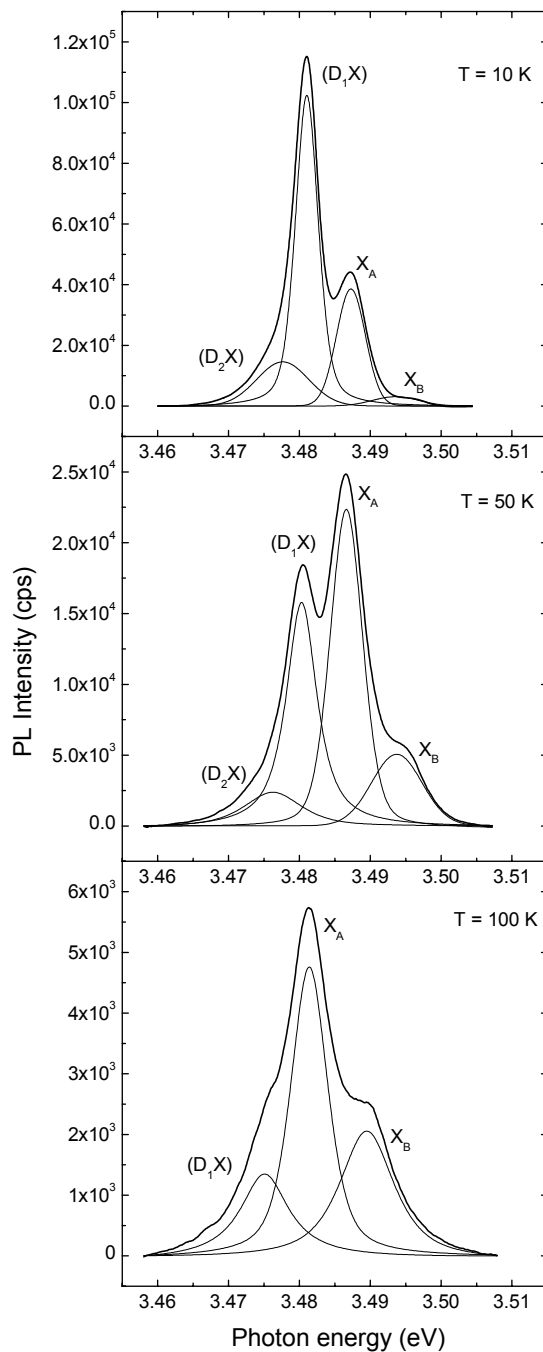


Fig. 2. The decomposition of the GaN-layer luminescence spectrum at different temperatures.

can conclude that the stresses in our GaN layers are of about 0.5 GPa. or 0.25 GPa if one uses the first or the second value, respectively. These stresses influence considerable the PL and PR excitonic spectra. Apart from a shift, the PL peaks are broadened in comparison with the non-stressed layers [10,29]. The reflectivity contours are as well deformed. The separation between the maximum and minimum

in the exciton reflectivity spectra in stressed layers is about 6 meV (in contrast with  $\sim 1$  meV in non-stressed layers [10,29]). Several reasons for such a difference can be considered: (i) strain increased L-T splitting; (ii) stress increased damping parameter; (iii) non-uniform distribution of strains across the layer. However, the first reason is less probable, since the L-T splitting is an indicative of the oscillator strength, while the peak-to-peak amplitude of the exciton resonance in the reflectivity spectra of our layers is about 8 % against 40 % in non-stressed layers [29].

The splitting between the A, B, and C excitons is as well different from that in non-stressed material. According to [10,22,29], the  $X_B^{n=1} - X_A^{n=1}$  splitting is 5 meV, and the  $X_C^{n=1} - X_A^{n=1}$  splitting equals 22 meV in a non-stressed layer. In our case, the  $\Delta E_{BA}$  and  $\Delta E_{CA}$  splitting is about 8 meV and 35 meV, respectively. These values are consistent with the previously reported splitting of  $8 \pm 1$  meV and  $30 \pm 5$  meV for similarly stressed GaN layers [22]. The scatter in the experimentally determined splitting was explained [22] (i) by the partial violation of the 1:1 connection assumed between hydrostatic and shear strain, and (ii) by the fact that any partial, anisotropic relaxation would occur differently for each sample represented in a set of dissimilar samples. One can observe that, in spite of nonlinearity in the  $\Delta E_{BA}$  and  $\Delta E_{CA}$  dependence on strain [22], the ratio  $\Delta E_{BA}/\Delta E_{CA}$  remains practically constant and equals 0.23 for the diapason of strains really inherent to GaN layers grown on sapphire substrates.

On the other hand, the separation between  $n=1$  and  $n=2$  for A and B excitons estimated from Fig. 2 is  $\sim 20$  meV, implying a binding energy of  $\sim 26$  meV. This value correlates with the binding energy of A and B excitons determined for non-stressed GaN material [10,16,26,29] proving the independence of the binding energy on strain.

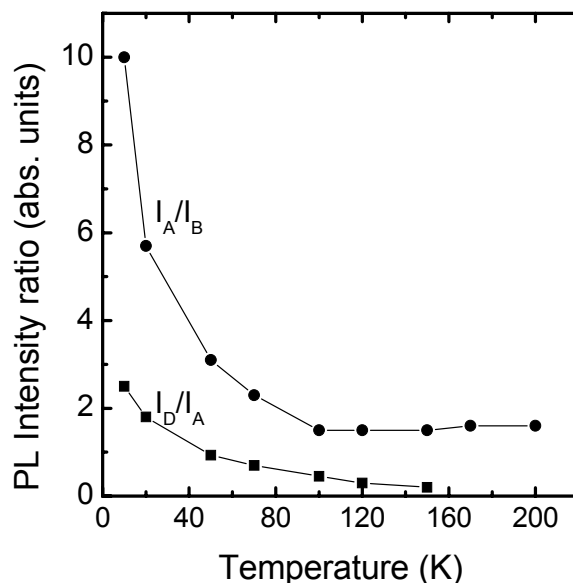


Fig. 3. Temperature dependence of the PL intensity ratio for the A exciton to B exciton (circle symbols), and bound exciton to A exciton (square symbols).

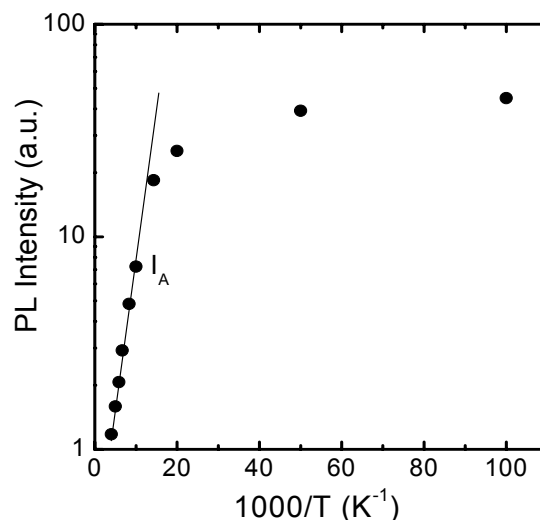


Fig. 4. Temperature dependence of the A exciton PL intensity.

With increasing temperature the PL intensity is redistributed in the favor of free exciton emission against bound exciton from one side, and in the favor of B exciton against A exciton from the other side (see Figs 2 and 3). This is consistent with the previous observations accounted for long lifetime in “bottleneck” states [29,30] leading to an enhanced emission of higher energy excitons. From the slope of the straight line in Fig. 4, the activation energy of the A and B excitons is estimated as 26 meV. This value coincides with the free exciton binding energy deduced from the separation between the ground and the first excited states, which is one more evidence of the independence of exciton binding energy on strains.

## CONCLUSION

In the investigated AlN/GaN/sapphire heterostructures the luminescence from the GaN channel layer is excitonic. In spite of growing a ~20 nm thick GaN nucleation layer between the sapphire substrate and GaN layer, the exciton peaks are blue shifted by about 10 meV in comparison with non-stressed material due to the remaining strains. The  $\Delta E_{BA}$  and  $\Delta E_{CA}$  exciton splitting is increased by a factor of 8/5. The activation energy of the A and B excitons equals 26 meV, it being independent of strains.

*Acknowledgement* This work was supported by CRDF and MRDA under Grant # ME2-3013.

## References

1. Nakamura S., Senoh M., Iwasa N., and Nagahama S., Jpn. J. Appl. Phys. **34**, Part. 2, L797 (1995).
2. Nakamura S., Senoh M., Nagahama S., Iwasa N., Yamada T., Matsushita T., Sagimoto Y., and Kiyoku H., Jpn. J. Appl. Phys. **36**, Part. 2, L1059 (1997).
3. Khan M.A., Kuznia J.N., Olson D.T., Schaff W.J., Burm J.W., and Shur M.S., Appl. Phys. Lett. **65**, 1121 (1994).
4. Zopler J.C., Shul R.J., Baca A.G., Wilson R.G., Pearton S.J., and Stall R.A., Appl. Phys. Lett. **68**, 2273 (1996).

5. Kawai H., Hara M., Nakamura F., Imanaga S., *Elect. Lett.* **34**, 592 (1998).
6. Alekseev E., Eisenbach A., Pavlidis D., 23<sup>th</sup> Workshop on Compound Semiconductors Devices and Integrated Curcuits, Chantilly, France, May 1999.
7. For instance, see Thijs P.J.A., Tiemeijer L.F., Kuindersma P.I., Binsma J.J.M., Dongen T.V., *IEEE J. Quantum Electron.* **27**, 1426 (1991), and references therein.
8. Aumer M.E., LeBoeuff S.F., Bedair S.M., Smith M., Lin J.Y., Jiang H.X., *Appl. Phys. Lett.* **77**, 821 (2000).
9. Skromme B.J., in Edited by: P.H. Holloway, G.E. McGuire, (Noyes, New Jersey, 1995) 678-771.
10. Scromme B.J., *MRS Internet J. Nitride Semicond. Res.* **4**, 15 (1999).
11. Kamiyama S., Ohnaka K., Suzuki M., Uenoyama T., *Jpn. J. Appl. Phys* **34**, Part. 2, L821 (1995).
12. Nido M., *Jpn. J. Appl. Phys.* **34**, Part. 2, L1513 (1995).
13. Majewski J.A., Stadele M., Vogl P., *MRS Internet J. Nitride Semicond. Res.* **1**, 30 (1996).
14. Gil B., Briot O., Aulombard R.L., *Phys. Rev. B* **52**, R17028 (1995).
15. Gil B., Hadani F., Morkoc M., *Phys. Rev. B* **54**, 7678 (1996).
16. Shikanai A., Azuhata T., Sota T., Chichibu S., Kuramata A., Horino K., Nakamura S., *J. Appl. Phys.* **81**, 417 (1997).
17. Gil B., *Semiconductors and Semimetals*, edited by Pankove J.I. and Moustakas T.D. (Academic, San Diego, 1999), vol. 57, p. 209.
18. Orton J.W., *Semicond. Sci. Technol.* **11**, 1026 (1996).
19. Orton J.W., *Semicond. Sci. Technol.* **12**, 64 (1997).
20. Shan W., Schmidt T.J., Hauenstein R.J., Song J.J., Goldenberg B., *Appl. Phys. Lett.* **66**, 3492 (1995).
21. Rieger W., Metzger T., Angerer H., Dimitrov R., Ambacher O., Stutzmann M., *Appl. Phys. Lett.* **68**, 970 (1996).
22. Edwards N.V., You S. D., Bremser M.D., Weeks T.W., Nah O.H., Davis R.F., Liu H., Stall R.A., Horton M.N., Perkin N.R., Kuech T.F., Aspnes D.E., *Appl. Phys. Lett.* **70**, 2001 (1997).
23. Lee I.H., Choi I.H., Lee C.R., Noh S.K., *Appl. Phys. Lett.* **71**, 1359 (1997).
24. Davydov V. Yu., Averkiev N.S., Goncharuk I.N., Nelson D.K., Nikitina I.P., Polkovnikov A.S., Smirnov A.N., Jacobson M.A., Semchinova O.K., *J. Appl. Phys.* **82**, 5097 (1997).
25. Skromme B.J., Jayapalan J., Vaudo R.P. , Phanse V.M., *Appl. Phys. Lett.* **74**, 2358 (1999).
26. Yamaguchi A.A., Mochizuki Y., Sunakawa H., Usui A., *J. Appl. Phys.* **83**, 4542 (1998).]
27. Sim G.G., Yu P.W., Reynolds D.C., Look D.C., Kim S.S., Noh D.Y., *Mat. Res. Symp. Proc.* **693**, 13.33.1 (2002).
28. Eisenbach A., Pavlidis D., Bru-Chevallier C., Dubois C., and Guillot G., *Proc. 24<sup>th</sup> International Symposium on Compound Semiconductors (ISCS '97)*, San Diego, CA, pp. 219-222, September 7-11, 1997
29. Kornitzer K., Ebner T., Grehl M., Thonke K., Sauer R., Kirchner C., Schwegler V., Kamp M., Leszczynski M., Grzegory I., Porowski S., *Phys. Stat. Sol. (b)* **216**, 5 (1999).
30. Klingshirn C.F., *Semiconductor Optics*, Springer-Verlag, Berlin 1997, and references therein.